TECHNICAL MEMORANDUM

96

General circulation diagnostics package

Guo xiong Wu and C Brankovic

Research Department

January 1985

European Centre for Medium-Range Weather Forecasts
Europäisches Zentrum für mittelfristige Wettervorhersage
Centre européen pour les prévisions météorologiques à moyen

CONTENTS

1. INTRODUCTION

A package has been designed to calculate the transfer properties of both eddies and mean meridional circulations, the budgets of angular momentum, heat and water, and the mean meridional mass flux of the atmosphere. These calculations are available for either analyses or numerical experiments. The corresponding difference fields between two experiments, two analyses or between experiment and analysis can also be evaluated. Results are presented in the form of height-latitude cross-sections which can be produced in the form of table or as graphical output.

2. FORMULATIONS

2.1 The mean meridional mass flux

In a system with pressure as vertical coordinate, the zonal mean continuity equation can be written as

$$\frac{\partial}{\partial p}(\bar{\omega}\cos\phi) + \frac{1}{a}\frac{\partial}{\partial\phi}(\bar{v}\cos\phi) = 0 \qquad (1)$$

where the overbar denotes the time and zonal mean, and other symbols have their usual meteorological meaning unless indicated otherwise. The zonal mean flux of mass X can be defined by the following pair of equations

$$\frac{2\pi a^2}{g}\bar{\omega}\cos\phi = -\frac{\partial X}{\partial\phi} = -A \qquad (2)$$

$$\frac{2\pi a}{g}\bar{v}\cos\phi = \frac{\partial X}{\partial p} = B \qquad (3)$$

Since the Euler condition

$$\frac{\partial A}{\partial p} - \frac{\partial B}{\partial\phi} = 0$$

is satisfied, X is an analytical function of ϕ and p which can be expressed as

$$dX = \left(\frac{\partial X}{\partial\phi}\right)d\phi + \left(\frac{\partial X}{\partial p}\right)dp \qquad (4)$$

and the integration of X is independent of path.

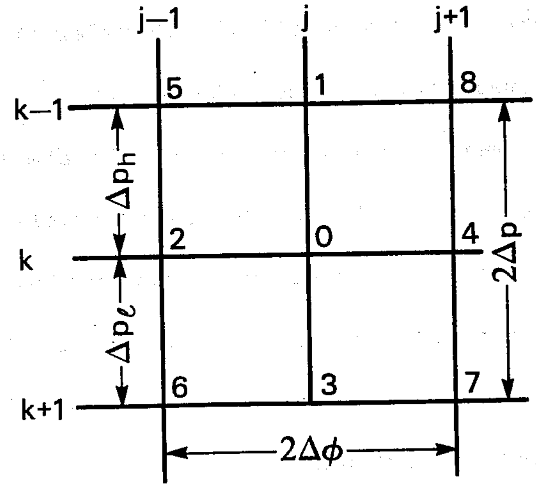

Fig. 1 Grid used to calculate the mean meridional mass flux

With the aid of Fig. 1 we see that the value of X at gridpoint 0(j,k) can be obtained from that at point 5(j-1,k-1) through either of the following line integrations

$$X_0 = X_5 + A_{15}\,\Delta\phi + B_{10}\Delta p_h \tag{5}$$

$$X_0 = X_5 + A_{20}\,\Delta\phi + B_{52}\Delta p_h \tag{6}$$

where $A_{mn} = (A_m+A_n)/2$ and $B_{mn} = (B_m+B_n)/2$ represent mean quantities in the line integrations in the meridional and vertical directions respectively. Taking the mean of (5) and (6), we then have

$$X_0 = X_5 + 0.25(A_5+A_1+A_2+A_0)\,\Delta\phi + 0.25(B_5+B_1+B_2+B_0)\,\Delta p_h \tag{7}$$

Applying a similar expression to that of (7) for the other diagonal surrounding points 6(j-1,k+1), 7(j+1,k+1) and 8(j+1,k-1), and taking the mean gives

$$X_{j,k} = 0.25(X_{j+1,k+1} + X_{j-1,k+1} + X_{j+1,k-1} + X_{j-1,k-1}) + G_{j,k}\,(\dot{\omega},\dot{v},\phi,p) \tag{8}$$

where

$$G_{j,k}(\bar{\omega},\bar{v},\phi,p) = 0.0625\ \{\Delta\phi[(A_7+2A_4+A_8)-(A_5+2A_2+A_6)]$$
$$-[\Delta p_\ell(B_6+B_7+B_2+B_4+2B_3+2B_0)-\Delta p_h(B_5+B_8+B_2+B_4+2B_1+2B_0)]\} \qquad (9)$$

Eq. (8) can be solved by an iterative method. The required $\bar{\omega}$ and $\bar{v}$ fields can be retrieved either from an analysis or from an experiment. In the vertical, standard pressure levels from 30 mb to 1000 mb are used. In the horizontal, data are spaced every three degrees of latitude from 87°N to 87°S. The boundary conditions used in the calculations are X=0 at the upper boundary (p=0) and at the poles since there is no net mass flux at these places. At 1000 mb X may be obtained by using either (2) or (3), and experiments show that the results are not very sensitive to which one is chosen. In the program described here, (2) is used to obtain the lower boundary values via an iterative scheme.

2.2 Budgets of angular momentum, heat and water

For the rectangular grid box $\Delta\phi\Delta p$ shown in Fig. 1, the budget equation of angular momentum can be expressed as

$$2\pi a^3\cos^2\phi\left(\frac{\partial\bar{u}}{\partial t}\right)_{j,k} + 2\pi a^2[(\overline{uv}\cos^2\phi)_{j+1,k}-(\overline{uv}\cos^2\phi)_{j-1,k}]\frac{\Delta p}{2g}$$
$$+ 2\pi a^3[(\overline{u\omega}\cos^2\phi)_{j,k+1} - (\overline{u\omega}\cos^2\phi)_{j,k-1}]\frac{\Delta\phi}{2g}$$
$$- 4\pi a^3\Omega\ (\bar{v}\sin\phi\cos^2\phi)_{j,k}\frac{\Delta\phi\Delta p}{g}$$
$$= -2\pi a^2[\Sigma\ (\phi_E-\phi_W)\cos\phi]_{j,k}\frac{\Delta\phi\Delta p}{g} - 2\pi a^3\ (F\cos^2\phi)_{j,k}\frac{\Delta\phi\Delta p}{g} + S$$
$$\equiv R_a \qquad (10)$$

where the first three terms on the left hand side denote the spin-up, and the horizontal and vertical divergence of angular momentum; the fourth term denotes the negative inertial torque of the mean meridional circulation exerted upon the atmosphere (its vertical component has been neglected since it is very small). On the right hand side, the first two terms represent the mountain torque and the surface frictional torque, and the third term represents the other kinds of sources and sinks of angular momentum (such as those due to small scale turbulences and gravity waves). These three terms on the right hand side are then defined as the sources of angular momentum R_a. In the following calculations, R_a is computed as the sum of all terms on the left hand side.

The heat budget in a rectangular grid box $\Delta\phi\Delta p$ can be expressed as

$$2\pi a^2 c_p \left(\cos\phi \frac{\partial \bar{T}}{\partial t}\right)_{j,k} \frac{\Delta\phi\Delta p}{g} + 2\pi a c_p [(\overline{vT}\cos\phi)_{j+1,k} - (\overline{vT}\cos\phi)_{j-1,k}] \frac{\Delta p}{2g}$$

$$+ 2\pi a^2 c_p [(\overline{\omega T}\cos\phi)_{j,k+1} - (\overline{\omega T}\cos\phi)_{j,k-1}] \frac{\Delta\phi}{2g}$$

$$- 2\pi a^2 (\alpha\bar{\omega})_{j,k} \frac{\Delta\phi\Delta p}{g}$$

$$= 2\pi a^2 (Q\cos\phi)_{j,k} \frac{\Delta\phi\Delta p}{g} \equiv R_T \qquad (11)$$

The four terms on the left hand side represent the local rate of change of mean temperature $\bar{T}$ with time ('warm-up'), the heat divergence in the horizontal and in the vertical, and the adiabatic cooling resulting from the vertical motions of the toroids (mean meridional circulation). The residual R_T is defined as the sum of all these terms; this represents the diabatic heating in the atmosphere.

The water budget can be expressed as

$$2\pi a^2 (\cos\phi \frac{\partial \bar{q}}{\partial t})_{j,k} \frac{\Delta\phi\Delta p}{g} + 2\pi a[(\overline{vq}\cos\phi)_{j+1,k} - (\overline{vq}\cos\phi)_{j-1,k}] \frac{\Delta p}{2g}$$

$$+ 2\pi a^2 [(\overline{\omega q}\cos\phi)_{j,k+1} - (\overline{\omega q}\cos\phi)_{j,k-1}] \frac{\Delta\phi}{2g}$$
$$= 2\pi a^2 (S\cos\phi)_{j,k} \frac{\Delta\phi\Delta p}{g} \equiv R_q \qquad (12)$$

The three terms on the left hand side represent the local rate of change with time of mean specific humidity $\bar{q}$ ('moist-up'), and the water divergence in the horizontal and in the vertical. The residual R_q is defined as the sum of all these terms, and it represents the water sources and sinks in the atmosphere.

The second and third terms on the right hand sides of the all above budget equations, representing the horizontal and vertical divergences of quantities, are decomposed into contributions from toroids, and from eddies in different wavenumber bands. The following schemes are employed in calculating divergence terms at inner grid points:

$$(\frac{\partial A}{\partial \phi})_{j,k} = [\frac{1}{2} (A_{j+1,k} + A_{j,k}) - \frac{1}{2} (A_{j,k} + A_{j-1,k})] \frac{1}{\Delta\phi}$$
$$= \frac{(A_{j+1,k} - A_{j-1,k})}{2\Delta\phi} \qquad (13)$$

$$(\frac{\partial A}{\partial p})_{j,k} = [\frac{1}{2} (A_{j,k+1} + A_{j,k}) - \frac{1}{2} (A_{j,k} + A_{j,k-1})] \frac{1}{\frac{1}{2}(p_{k+1} - p_{k-1})}$$
$$= \frac{(A_{j,k+1} - A_{j,k-1})}{2\Delta p_k} \qquad (14)$$

At the lower boundary (level k), the vertical difference is calculated by using

$$(\frac{\partial A}{\partial p})_{j,k-\frac{1}{2}} = \frac{(A_{j,k} - A_{j,k-1})}{150} \qquad (15)$$

and the other terms are treated as the average of those at 850 mb and 1000 mb. Therefore, the calculated budgets at the lower boundary actually represents those at 925 mb level.

Again, the data required for the calculations are retrieved either from an analysis or from an experiment at standard pressure levels, ranging from 30 mb to 1000 mb, and at an interval of three degrees of latitude from 87°N to 87°S.

2.3 Profiles of vertically integrated transfers

Across a complete latitude "wall", the transfer of angular momentum, geopotential, heat, and water can be expressed as

$$\begin{aligned}
F_a &= \int_{30}^{1000} 2\pi a^2 \, (\overline{vu\cos\phi}) \, \frac{dp}{g} \\
F_g &= \int_{30}^{1000} 2\pi a \, (\overline{vz\cos\phi}) \, \frac{dp}{g} \\
F_T &= \int_{30}^{1000} 2\pi a \, (\overline{vT\cos\phi}) \, \frac{dp}{g} \\
F_q &= \int_{30}^{1000} 2\pi a^2 \, (\overline{vq\cos\phi}) \, \frac{dp}{g}
\end{aligned} \qquad (16)$$

The convergences of F_a , F_T and F_q in a latitude belt $\Delta\phi$ (three degrees in the present calculations) can be evaluated as

$$\begin{aligned}
C_a &= - \frac{\partial F_a}{\partial \phi} \Delta\phi \\
C_T &= - \frac{\partial F_T}{\partial \phi} \Delta\phi \\
C_q &= - \frac{\partial F_q}{\partial \phi} \Delta\phi
\end{aligned} \qquad (17)$$

These terms are also calculated using the centred difference scheme given in 13).

3. USER'S GUIDE TO THE PACKAGE

Fig. 2 depicts important program units within the package. The details are described in this section.

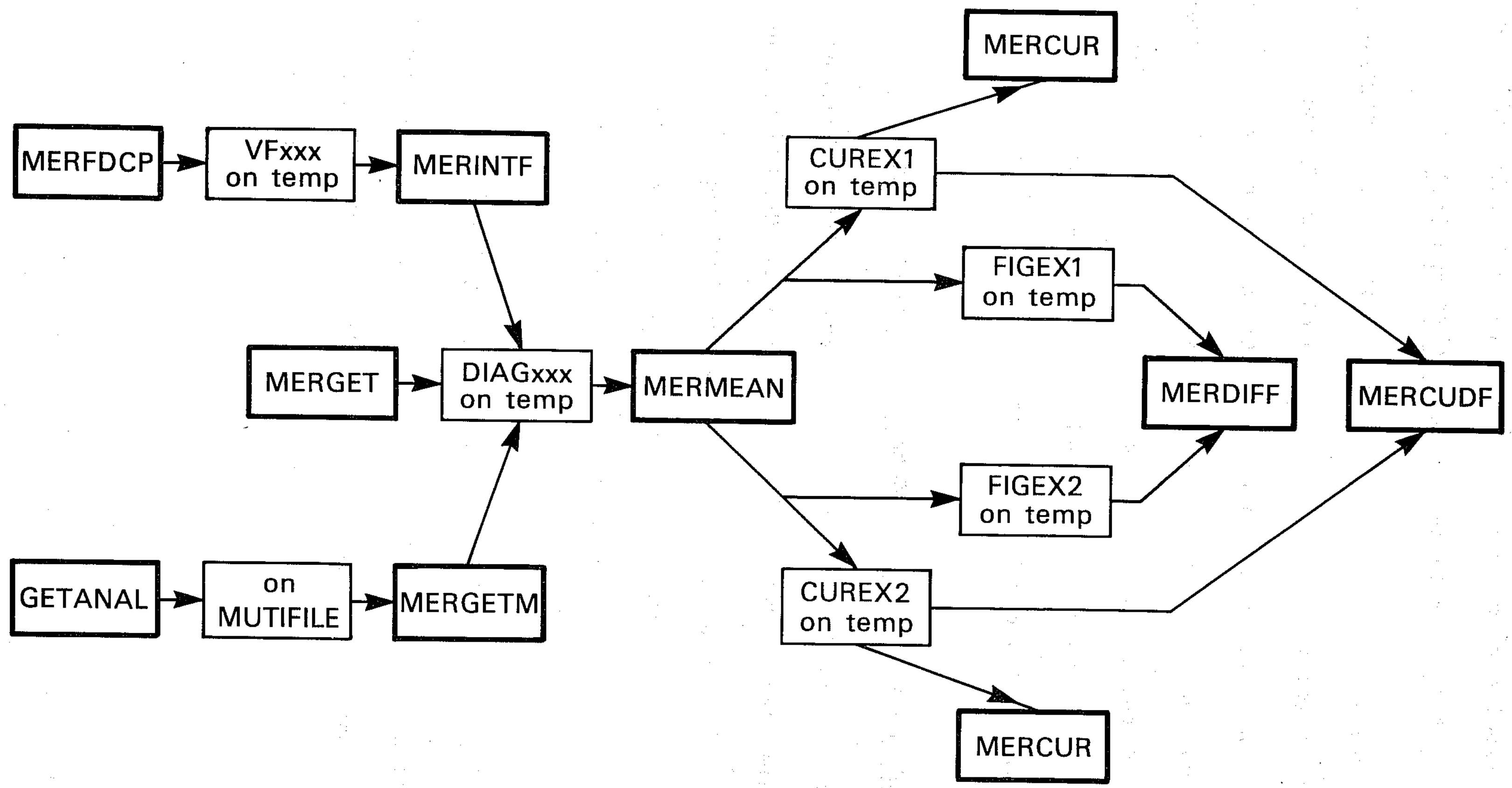

Fig.2 Flow diagram of the programs in the package.

3.1 Data retrieval

One of the following three steps is necessary to retrieve the required data.

(a) GETANAL and MERGETM (data from the ECMWF archive)

GETANAL is designed to retrieve archived data through the GETDATA procedure. It extracts u, v (or vorticity and divergence), ω, z, T, and q (or relative humidity) and then writes them to a mutifile tape. The interface program MERGETM fetches those data from the tape and calculates the Fourier coefficients of various diagnostic quantities. Results are written to the file named DIAGxxx, where "xxx" stands for the experiment name given by the user. File DIAGxxx is cataloged to the public pack 'temp'.

(b) MERFDCP and MERINTF (FIND data from a research experiment)

For experimental results originating from the Research Department under the experiment name "xxx", MERFDCP (which is based on the FIND procedure) searches for those results and copies the required data to the 'temp' with file name VFxxx. Then the program MERINTF performs a similar role to that of MERGETM, i.e., after the successful exit, file DIAGxxx is written to the 'temp'.

(c) MERGET (other data from a research experiment)

If experimental results in the form of spherical harmonics coefficients reside at any particular tape, MERGET retrieves those results, calculates Fourier coefficients, and stores them to DIAGxxx on 'temp' providing the tape 'vsn' is known.

For above programs MERGET, MERGETM and MERINTF, the user would specify

(i) number of unwanted files to be skipped (if any).

(ii) number of files to be scanned.

(iii) u and v or vorticity and divergence, and q or relative humidity, depending on the input data categories.

(iv) time interval of the data available from the data store.

3.2 Program MERMEAN to calculate and plot output data

This is the core of the package. It retrieves the file DIAGxxx from 'temp', selects the required data, performs all the calculations, and plots all cross-sections. Before submitting the job, the following specifications are required:

(i) name of the data file DIAGxxx stored on 'temp'.

(ii) number of files nn required for the time-mean calculations; this can be fulfilled by changing the parameter NTIM=11 to NTIM=nn throughout the program.

(iii) one 16-character line located two lines from the end of the program, giving the information the user wishes to print out at the top of data tables.

(iv) one 40-character line located next to the last line of the program, indicating the title the user wishes to have at the top of each figure.

(v) one 5-digit floating point number located at the end of the program, indicating the time interval of the retrieved data in units of hours.

The following three groups of latitude-height cross-sections are available from the program (see the Appendix):

(a) Time-mean fields: $\bar{u}$, $\bar{v}$, $\bar{\omega}$, $\bar{z}$, $\bar{T}$, $\bar{q}$, and mass flux X; the transfer properties of $\overline{vu}$, $\overline{\omega u}$, $\overline{vz}$, $\overline{\omega z}$, $\overline{vT}$, $\overline{\omega T}$, $\overline{vq}$ and $\overline{\omega q}$ due to both toroids and eddies in different wavenumber bands.

(b) Vector-form fields of $(\bar{v},\bar{w})$, $(\overline{vu},\overline{wu})$, $(\overline{vz},\overline{wz})$, $(\overline{vT},\overline{wT})$ and $(\overline{vq},\overline{wq})$ due to both toroids and eddies in different wavenumber bands.

(c) Budgets of angular momentum, sensible heat and water.

After a successful exit, the program launches two pieces of data FIGxxx and CURxxx stored on 'temp' again. FIGxxx is used for later comparisons (see Sect. 3.4), while CURxxx contains all the information about the vertical integrations.

3.3 Plotting program MERCUR

This program retrieves data CURxxx from the 'temp' disc and plots the transfer profiles F_a, F_g, F_T and F_q (see (16)) and the convergence profiles C_a, C_T and C_q (see (17)). In order to run this program, the data title CURxxx must be specified.

3.4 Comparison program MERDIFF

MERDIFF calculates the difference between two fields from different origins and generates the same categories of output as described in Sect. 3.2. Upon entry the program retrieves two pieces of data DIAGex1 and DIAGex2 from 'temp'. The difference between them (DIAGex1-DIAGex2) is calculated before a procedure similar to MERMEAN is executed. All the specifications listed in Sect. 3.2 are therefore required. Similar outputs to these from MERMEAN, but for the difference fields, are available from this program.

3.5 Comparison program MERCUDF

MERCUDF calculates the difference between two sets of transfer profiles which were obtained from program MERCUR. Initially the program retrieves two pieces of data CURex1 and CURex2 from 'temp'. The difference between them (CURex1-CURex2) is calculated before a procedure like MERCUR (see Sect. 3.3) is executed. In order to run this program, therefore, the data titles CURex1 and CURex2 must be specified.

4. MAGNITUDES AND CONTOURING INTERVALS

The order of magnitude and intervals of the contour charts are automatically adjusted by the package, and usually give a satisfactory appearance. However, if one wishes to change the intervals or magnitudes of the output, then simply change the parameter NUMBOR and/or NUMBIN in program MERMEAN and/or MERDIFF to 99. Then specifications of the required values for magnitude array ORDER and the interval array CINT are needed in the following subroutines:

subroutine CRSMAP	if NUMBOR≠99, default NUMBOR=02;
subroutine VECFLUX	if NUMBOR≠99, default NUMBOR=01;
subroutine BUDGET	if NUMBOR≠99, default NUMBOR=02.

The arrays ORDER and CINT are assigned by DATA statements in a sequential order corresponding to that of the output contours as listed in the Appendix.

5. AN EXAMPLE

On the mutifile tape VSN=4673D, the 60-day forecast files from the ECMWF T21 model are stored. The initial day is 1 January, 1983 and the mean orography scheme is used. On another tape with VSN=18381V, results from a parallel experiment, but without orography, are stored. In order to understand the role of mechanical forcing in the atmosphere, the present package is used to compare their results. The two experiments are titled as MTN and NOM respectively. The last thirty days of the forecast are retrieved. The procedure is carried out as follows.

5.1 Attach programs

(a) ATTACH,WULIB,ID=NEW	Attach fileset which contains
(b) FS,WULIB	all required program units
(c) GF,MERGET	Get the programs
GF,MERMEAN	
GF,MERCUR	
GF,MERDIFF	
GF,MERCUDF	

5.2 Operate MERGET

(a) RS/XXXXXX/4673D/*,V	Specify tape VSN
(b) RS/XXX/MTN/,V	Specify experiment title
(c) NINT=24	Specify time interval (24 hours)
(d) NSCANF=30	Specify no. of files to be retrieved
(e) SKIPF,DN=FT03,NF=31.	Skip unwanted files (31 files since the first one is the analysis)

After job completion, data file DIAGMTN is stored to the 'temp'. Repeating the same procedure with VSN=18381V and title NOM will generate another file DIAGNOM on 'temp'.

5.3 Operate MERMEAN

(a)	RS/XXX/MTN/*,V	Specify experiment title
(b)	RS/NTIM=mm/NTIM=30/*,V	Specify no. of files to be executed
(c)	F*;F-3;D;I; *MTN*	Change title of output; this is a 16-character line described in Sect. 3.2 (iii).
(d)	F*;F-;D;I; T0=830101 T=0201-0302. NO.=MTN.	Change title for figures; this a is 40-character line (Sect. 3.2 (iv))

This job does all the calculations and produces cross-sections. Data sets FIGMTN and CURMTN are then written to the 'temp'. A similar job but with experiment name NOM (see (a), (c) and (d)), will perform the corresponding operations for the no mountain case; results FIGNOM and CURNOM are also stored to the 'temp'.

5.4 Operate MERCUR

In order to obtain vertically integrated fluxes of various quantities and the corresponding convergences, the experiment name XXX should be changed to MTN (or NOM).

5.5 Operate MERDIFF

(a)	RS/1/MTN/*,V RS/2/NOM/*,V	Specify experiment titles
(b)	RS/NTIM=mm/NTIM=30/*,V	Specify number of files to be executed

(c) F*;F-3;D;I; Change title of output

MTN-NOM

(d) F*;F-;D;I; Change title of figures

T0=830101 T=0201-0302. *MTN-NOM*

This job performs all the calculations and produces cross-sections for the difference fields. On exit, a data set MTNNOM is written to the 'temp'.

5.6 Operate MERCUDF

(a) RS/EX1/MTN/*,V Specify experiment title

RS/EX2/NOM/*,V

(b) F*;F-;D;I; Change title for figures

T0=830101 T=0201-0302. *MTN-NOM*

The vertically integrated difference fluxes of various quantities and their corresponding convergences are plotted as latitudinal profiles.

5.7 The output

When the package is used, the output consists of charts generated in subroutines CRSMAP, VEGFLUX, BUDGET and MERCUR. The plots from each of these are listed in parts A, B, C and D of the Appendix, and examples are given in Figs. A.1-A.14, Figs. B.1-B.5, Figs. C.1-C.7 and Figs. D.1-D.7.

Normally a complete set of charts is produced whenever the package is used.

ACKNOWLEDGEMENT

We would like to thank S.Tibaldi and K.Arpe for their helpful discussions during the design of the package, and to S.Uppala for his help in designing the plotting part of the package. Our thanks are also due to R.Riddaway for helping us to document the package

APPENDIX

Diagrams generated by the package

A. Diagrams generated by the subroutine CRSMAP

Time-mean fields: $\bar{u}$, $\bar{v}$, $\bar{\omega}$, $\bar{z}$, $\bar{T}$, $\bar{q}$, and mass flux X; the transfer properties of $\overline{vu}$, $\overline{\omega u}$, $\overline{vz}$, $\overline{\omega z}$, $\overline{vT}$, $\overline{\omega T}$, $\overline{vq}$ and $\overline{\omega q}$ due to both toroids and eddies in different wavenumber bands.

A1 Zonal mean zonal wind $\bar{u}$ (m/s) (Fig. A.1).

A2 Zonal mean meridional wind $\bar{v}$ (m/s).

A3 Zonal mean vertical wind $\bar{\omega}$ (mb/s).

A4 Zonal mean deviation from standard geopotential height $\bar{z}$ (gpm).

A5 Zonal mean temperature $\bar{T}$ (°C).

A6 Zonal mean specific humidity $\bar{q}$ (g/kg).

A7 Horizontal momentum flux by eddies with wave number 01-03 (m/s.m/s).

A8 Horizontal momentum flux by eddies with wave number 04-09 (m/s.m/s).

A9 Horizontal momentum flux by all eddies (m/s.m/s) (Fig. A.2).

A10 Horizontal momentum flux by toroids (m/s.m/s).

A11 Horizontal momentum flux by both eddies and toroids (m/s.m/s).

A12 Vertical momentum flux by eddies with wave number 01-03 (mb/s.m/s).

A13 Vertical momentum flux by eddies with wave number 04-09 (mb/s.m/s).

A14 Vertical momentum flux by all eddies (mb/s.m/s) (Fig. A.3).

A15 Vertical momentum flux by toroids (mb/s.m/s)

A16 Vertical momentum flux by both eddies and toroids (mb/s.m/s).

A17 Vertical geopotential flux by eddies with wave number 01-03 (mb/s.m^2/s^2).

A18 Vertical geopotential flux by eddies with wave number 04-09 (mb/s.m^2/s^2).

A19 Vertical geopotential flux by all eddies (mb/s.m2/s2) (Fig. A.4).

A20 Horizontal geopotential flux by eddies with wave number 01-03 ($m/s.m^2/s^2$).

A21 Horizontal geopotential flux by eddies with wave number 04-09 ($m/s.m^2/s^2$).

A22 Horizontal geopotential flux by all eddies ($m/s.m^2/s^2$) (Fig. A.5).

A23 Horizontal heat flux by eddies with wave number 01-03 (m/s.°K).

A24 Horizontal heat flux by eddies with wave number 04-09 (m/s.°K).

A25 Horizontal heat flux by all eddies (m/s.°K) (Fig. A.6).

A26 Horizontal heat flux by toroids (m/s.°K)

A27 Horizontal heat flux by both eddies and toroids(m/s.°K).

A28 Vertical heat flux by eddies with wave number 01-03 (mb/s.°K).

A29 Vertical heat flux by eddies with wave number 04-09 (mb/s.°K).

A30 Vertical heat flux by all eddies (mb/s.°K) (Fig. A.7).

A31 Vertical heat flux by toroids (mb/s.°K)

A32 Vertical heat flux by both eddies and toroids (mb/s.°K).

A33 Horizontal moisture flux by eddies with wave number 01-03 (m/s.g/kg).

A34 Horizontal moisture flux by eddies with wave number 04-09 (m/s.g/kg).

A35 Horizontal moisture flux by all eddies (m/s.g/kg) (Fig. A.8).

A36 Horizontal moisture flux by toroids (m/s.g/kg).

A37 Horizontal moisture flux by both eddies and toroids (m/s.g/kg).

A38 Vertical moisture flux by eddies with wave number 01-03 (mb/s.g/kg).

A39 Vertical moisture flux by eddies with wave number 04-09 (mb/s.g/kg).

A40 Vertical moisture flux by all eddies (mb/s.g/kg) (Fig. A.9).

A41 Vertical moisture flux by toroids (mb/s.g/kg).

A42 Vertical moisture flux by both eddies and toroids (mb/s.g/kg).

A43 Kinetic energy of eddies with wave number 01-03 ($10^2 J\ m^{-2} mb^{-1}$).

A44 Kinetic energy of eddies with wave number 04-09 ($10^2 J\ m^{-2} mb^{-1}$).

A45 Kinetic energy of all eddies (10^2J $m^{-2}mb^{-1}$) (Fig. A.10).

A46 Kinetic energy of the zonal flow (10^2J $m^{-2}mb^{-1}$).

A47 Total kenetic energy of eddies and the zonal flow (10^2J $m^{-2}mb^{-1}$).

A48 Potential energy of eddies with wave number 01-03 (10^2J $m^{-2}mb^{-1}$).

A49 Potential energy of eddies with wave number 04-09 (10^2J $m^{-2}mb^{-1}$).

A50 Potential energy of all eddies (10^2J $m^{-2}mb^{-1}$) (Fig. A.11).

A51 Zonal potential energy (10^2J $m^{-2}mb^{-1}$).

A52 Total potential energy (10^2J $m^{-2}mb^{-1}$).

A53 Energy conversion CE due to eddies with wave number 01-03 (10^{-4}W $m^{-2}mb^{-1}$).

A54 Energy conversion CE due to eddies with wave number 04-09 (10^{-4}W $m^{-2}mb^{-1}$).

A55 Energy conversion CE due to all eddies (10^{-4}W $m^{-2}mb^{-1}$) (Fig. A.12).

A56 Energy conversion CE due to toroids (10^{-4}W $m^{-2}mb^{-1}$).

A57 Energy conversion CE due to eddies and toroids (10^{-4}W $m^{-2}mb^{-1}$).

A58 Energy conversion CK due to eddies with wave number 01-03 (10^{-4}W $m^{-2}mb^{-1}$).

A59 Energy conversion CK due to eddies with wave number 04-09 (10^{-4}W $m^{-2}mb^{-1}$).

A60 Energy conversion CK due to all eddies (10^{-4}W $m^{-2}mb^{-1}$) (Fig. A.13)

A61 Energy conversion CA due to eddies with wave number 01-03 (10^{-4}W $m^{-2}mb^{-1}$).

A62 Energy conversion CA due to eddies with wave number 04-09 (10^{-4}W $m^{-2}mb^{-1}$).

A63 Energy conversion CA due to all eddies (10^{-4}W $m^{-2}mb^{-1}$) (Fig. A.14).

A64 Zonal mean mass flux X (10^6 ton/s).

B. Diagrams generated by the subroutine VECFLUX

Vector-form fields of $(\overline{v,w})$, $(\overline{vu},\overline{wu})$, $(\overline{vz},\overline{wz})$, $(\overline{vT},\overline{wT})$ and $(\overline{vq},\overline{wq})$ due to both toroids and eddies in different wavenumber bands.

B1 $(\bar{v},\bar{w})$ (Fig. B.1).

B2 $(\overline{vu},\overline{wu})$ by eddies with wave number 01-03.

B3 $(\overline{vu},\overline{wu})$ by eddies with wave number 04-09.

B4 $(\overline{vu},\overline{wu})$ by all eddies (Fig. B.2).

B5 $(\overline{vu},\overline{wu})$ by toroids.

B6 $(\overline{vu},\overline{wu})$ by both toroids and eddies.

B7 $(\overline{vz},\overline{wz})$ by eddies with wave number 01-03.

B8 $(\overline{vz},\overline{wz})$ by eddies with wave number 04-09.

B9 $(\overline{vz},\overline{wz})$ by all eddies (Fig. B.3).

B10 $(\overline{vT},\overline{wT})$ by eddies with wave number 01-03.

B11 $(\overline{vT},\overline{wT})$ by eddies with wave number 04-09.

B12 $(\overline{vT}, \overline{wT})$ by all eddies (Fig. B.4).

B13 $(\overline{vT}, \overline{wT})$ by toroids.

B14 $(\overline{vT}, \overline{wT})$ by both toroids and eddies.

B15 $(\overline{vq}, \overline{wq})$ by eddies with wave number 01-03.

B16 $(\overline{vq}, \overline{wq})$ by eddies with wave number 04-09.

B17 $(\overline{vq}, \overline{wq})$ by all eddies (Fig. B.5).

B18 $(\overline{vq}, \overline{wq})$ by toroids.

B19 $(\overline{vq}, \overline{wq})$ by both toroids and eddies.

C. Diagrams generated by the subroutine BUDGET

Budgets of angular momentum, sensible heat and water.

Abbreviations: AM- angular momentum;

Ht- sensible heat;

Wa- water contains;

HAM- horizontal angular momentum flux;

VAM- vertical angular momentum flux;

HHt- horizontal heat flux;

VHt- vertical heat flux;

HWa- horizontal water flux;

VWa- vertical water flux;

HDi- horizontal divergence;

VDi- vertical divergence;

C1 Spin-up of the zonal flow (Fig. C.1).

C2 HDi(HAM) due to eddies with wave number 01-03.

C3 HDi(HAM) due to eddies with wave number 04-09.

C4 HDi(HAM) due to all eddies (Fig. C.2).

C5 HDi(HAM) due to toroids.

C6 VDi(VAM) due to eddies with wave number 01-03.

C7 VDi(VAM) due to eddies with wave number 04-09.

C8 VDi(VAM) due to all eddies (Fig. C.3).

C9 VDi(VAM) due to toroids.

C10 Negative inertial torque.

C11 Angular momentum sources.

C12 Warm-up of the atmosphere in a latitude belt.

C13 HDi(HHt) due to eddies with wave number 01-03.

C14 HDi(HHt) due to eddies with wave number 04-09.

C15 HDi(HHt) due to all eddies (Fig. C.4).

C16 HDi(HHt) due to toroids.

C17 VDi(VHt) due to eddies with wave number 01-03.

C18 VDi(VHt) due to eddies with wave number 04-09.

C19 VDi(VHt) due to all eddies (Fig. C.5).

C20 VDi(VHt) due to toroids.

C21 Negative adiabatic heating.

C22 Heat sources.

C23 Moist-up of the atmosphere in a latitude belt.

C24 HDi(HWa) due to eddies with wave number 01-03.

C25 HDi(HWa) due to eddies with wave number 04-09.

C26 HDi(HWa) due to all eddies (Fig. C.6).

C27 HDi(HWa) due to toroids.

C28 VDi(VWa) due to eddies with wave number 01-03.

C29 VDi(VWa) due to eddies with wave number 04-09.

C30 VDi(VWa) due to all eddies (Fig. C.7).

C31 VDi(VWa) due to toroids.

C32 Water sources.

D. Diagrams generated by the subroutine MERCUR

D.1 Latitude profiles of vertically integrated horizontal fluxes

D1 Angular momentum flux (Fig. D.1).

D2 Geopotential flux (Fig. D.2).

D3 Heat flux (Fig. D.3).

D4 Water flux (Fig. D.4).

D.2 Latitude profiles of the vertical integrals of every single term in the budget equations

D5 Angular momentum budget (Fig. D.5).

D6 Heat budget (Fig. D.6).

D7 Water budget (Fig. D.7).

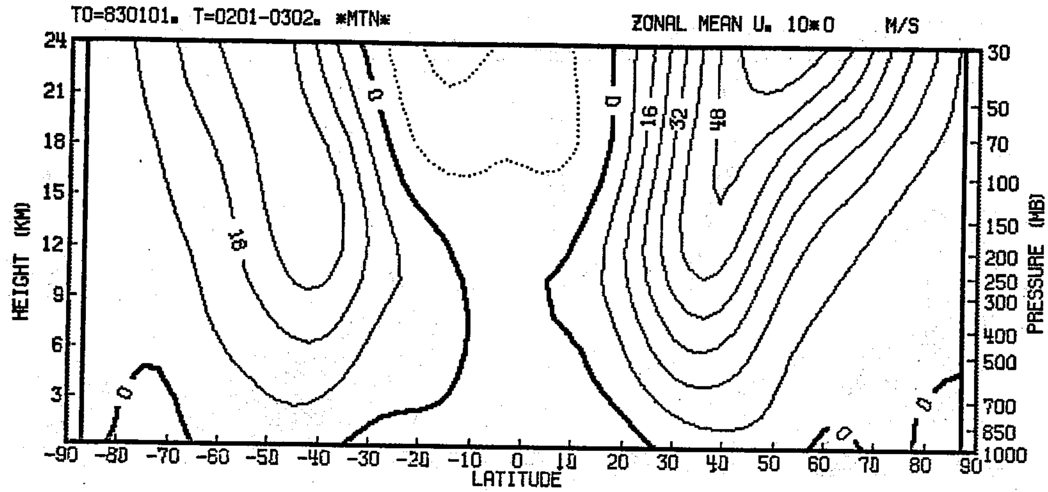

Fig. A.1 Zonal mean zonal wind [A1]

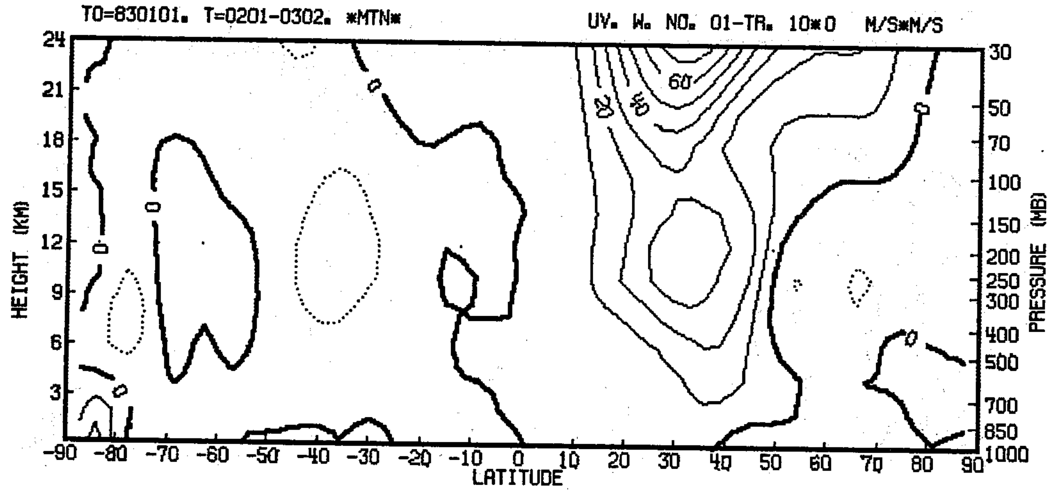

Fig. A.2 Horizontal momentum flux by all eddies [A9]

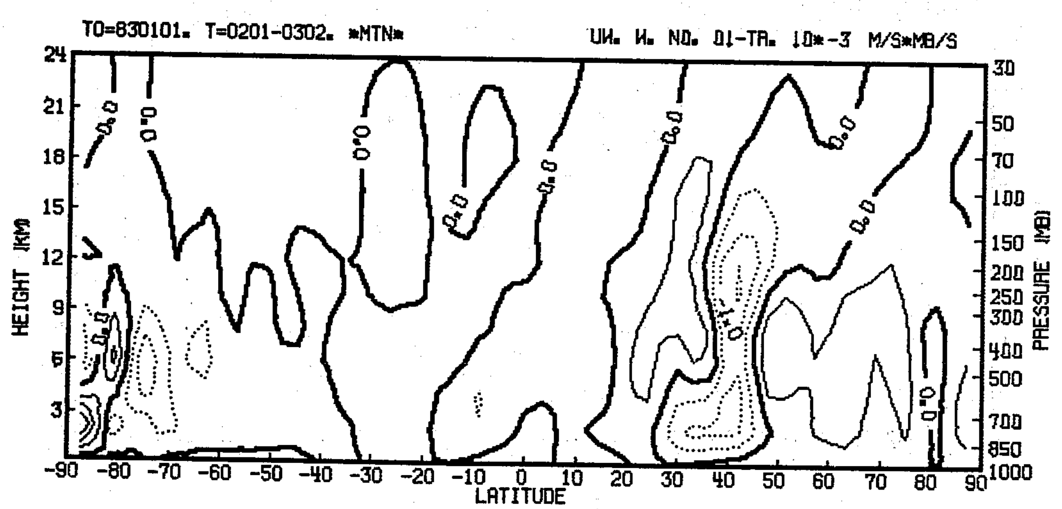

Fig. A.3 Vertical momentum flux by all eddies [A14]

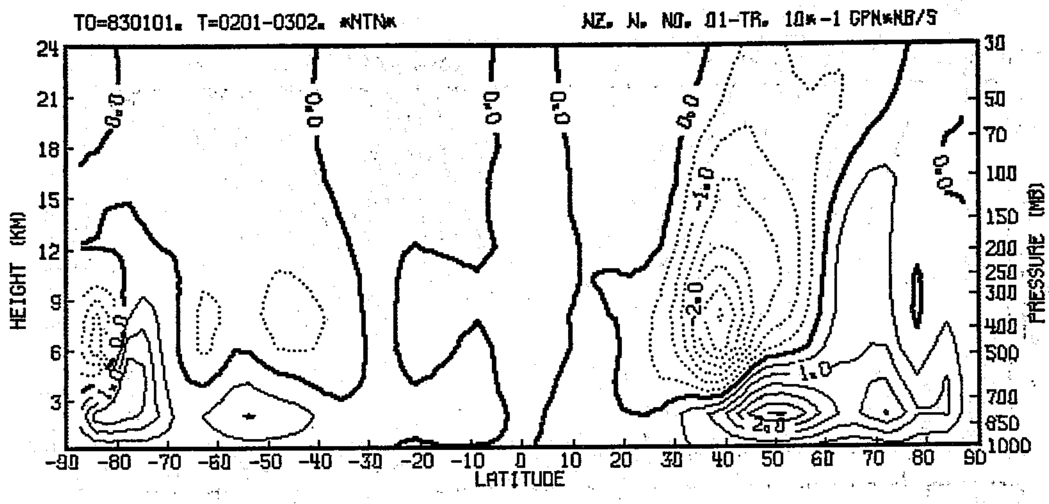

Fig. A.4 Vertical geoptential flux by all eddies [A19]

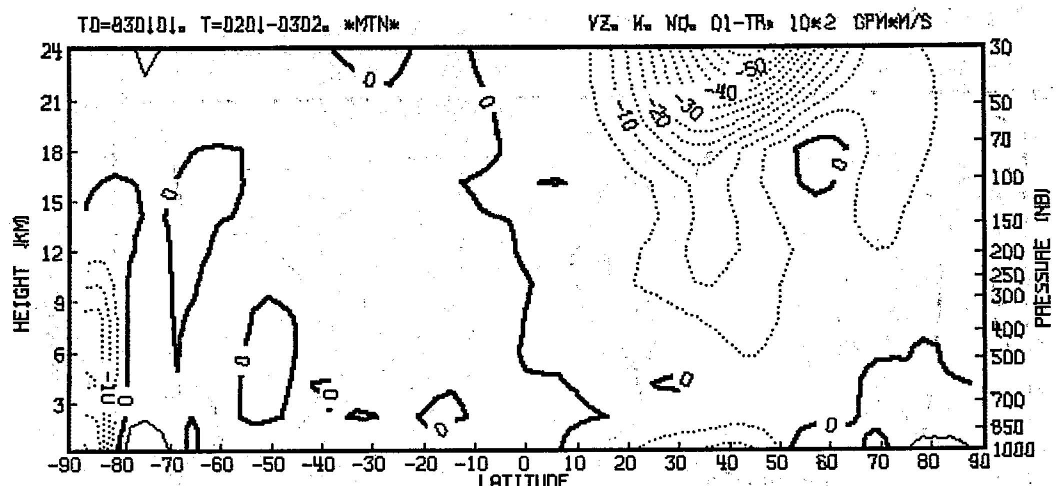

Fig. A.5 Horizontal geopotential flux by all eddies [A22]

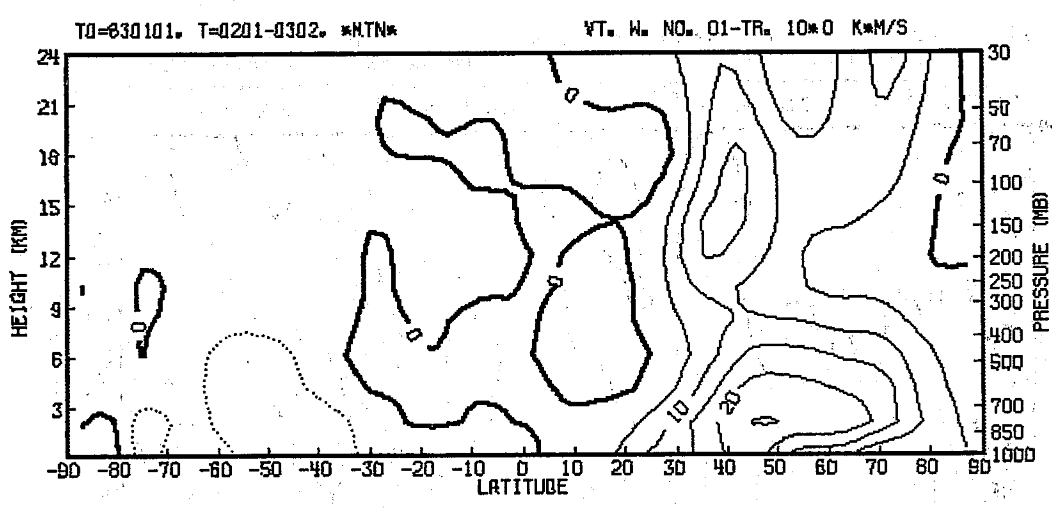

Fig. A.6 Horizontal heat flux by all eddies [A25]

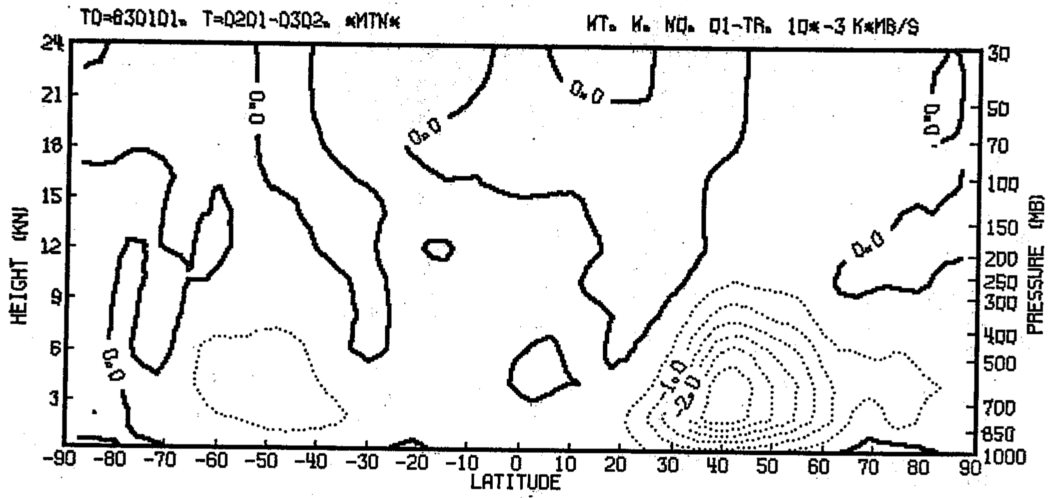

Fig. A.7 Vertical heat flux by all eddies [A30]

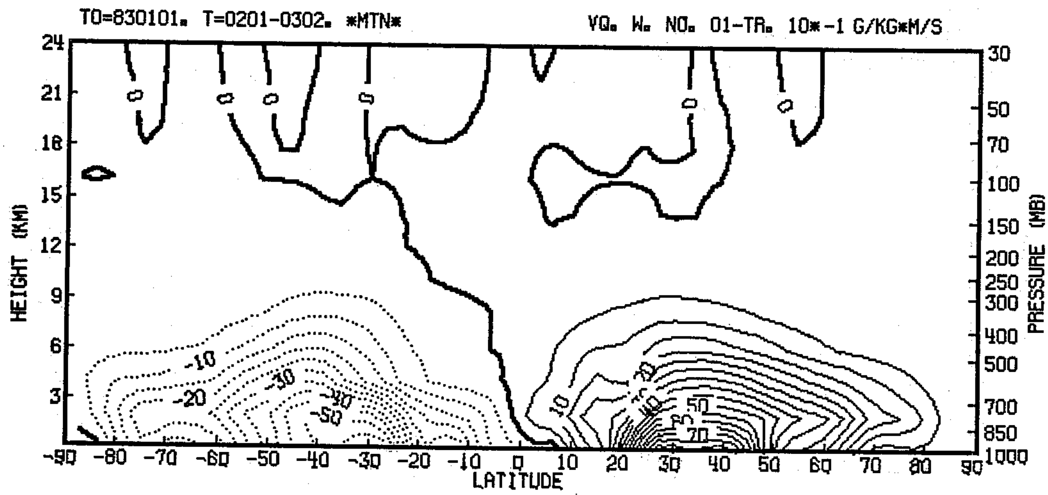

Fig. A.8 Horizontal moisture flux by all eddies [A35]

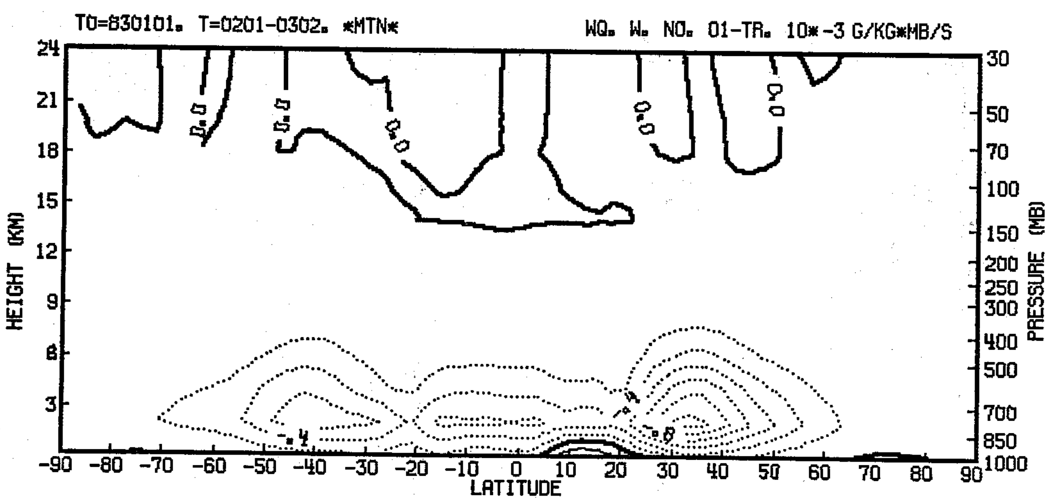

Fig. A.9 Vertical moisture flux by all eddies [A40]

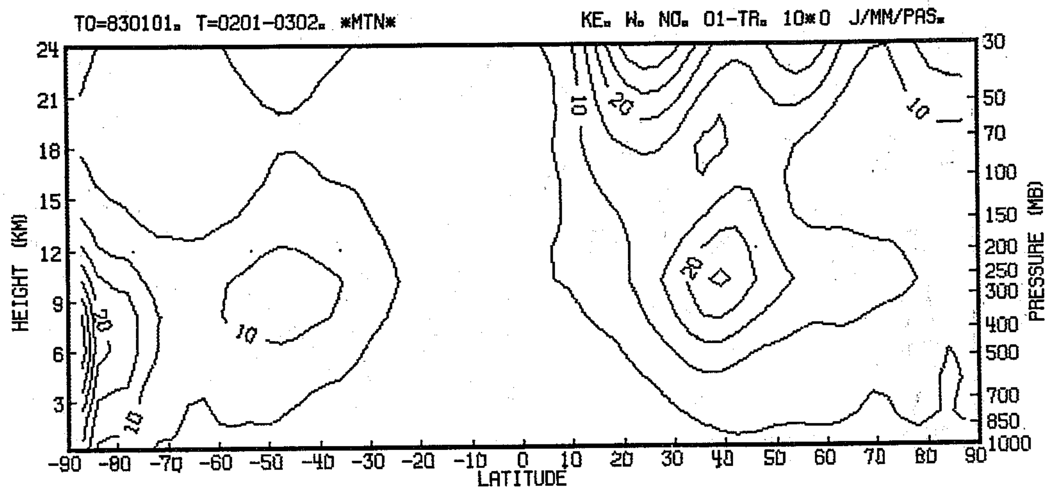

Fig. A.10 Kinetic energy of all eddies [A45]

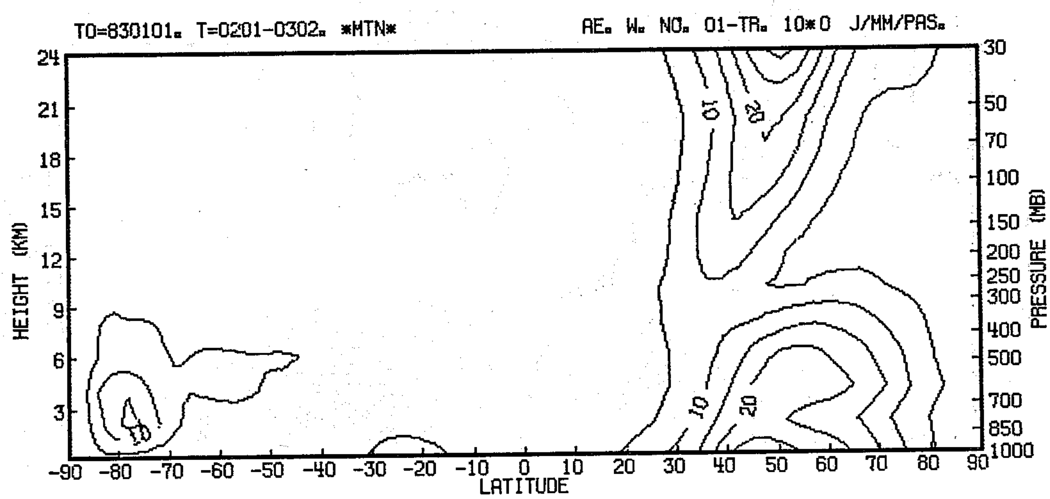

Fig. A.11 Potential energy of all eddies [A50]

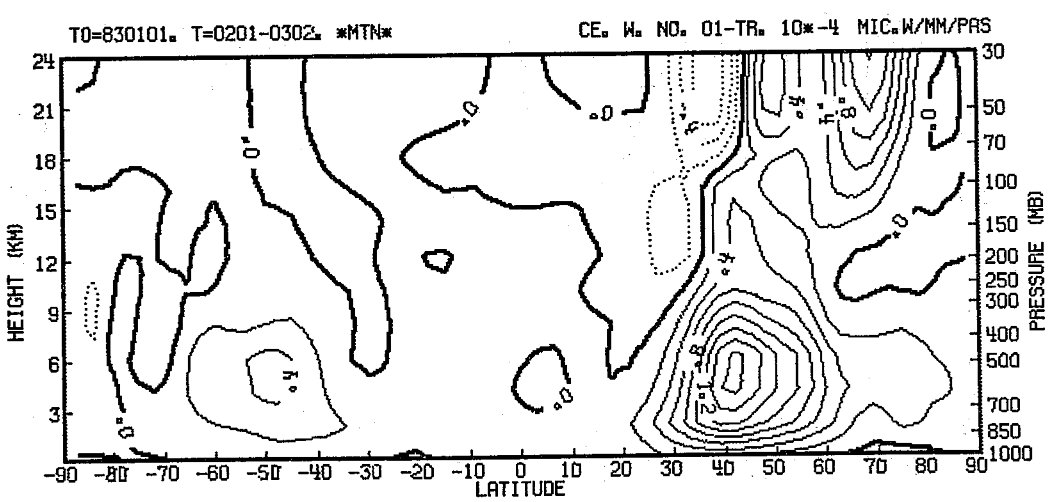

Fig. A.12 Energy conversion CE due to all eddies [A55]

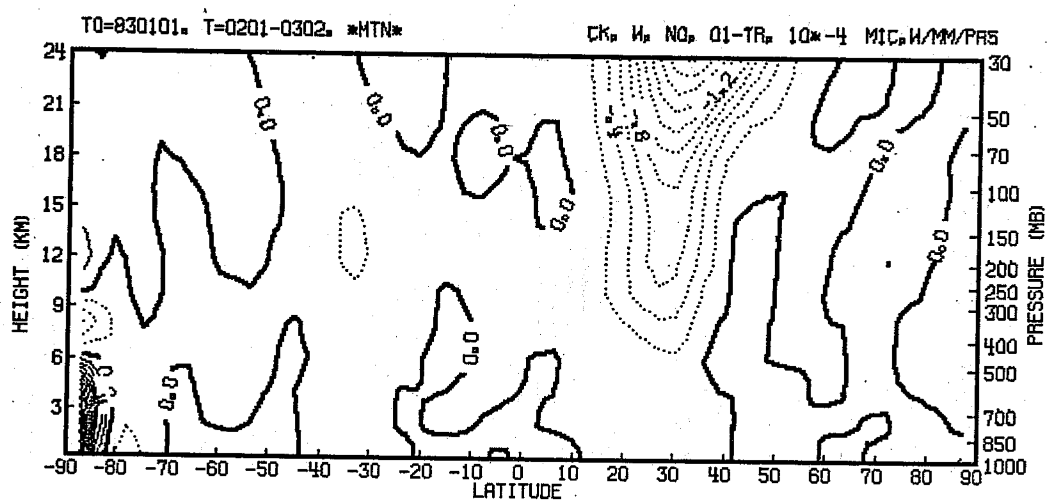

Fig. A.13 Energy conversion CK due to all eddies [A60]

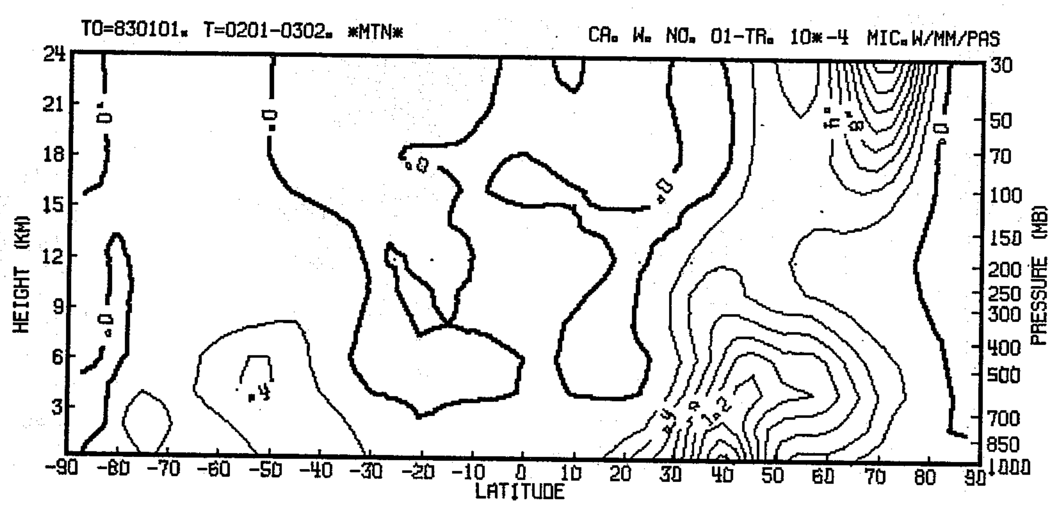

Fig. A.14 Energy conversion CA due to all eddies [A63]

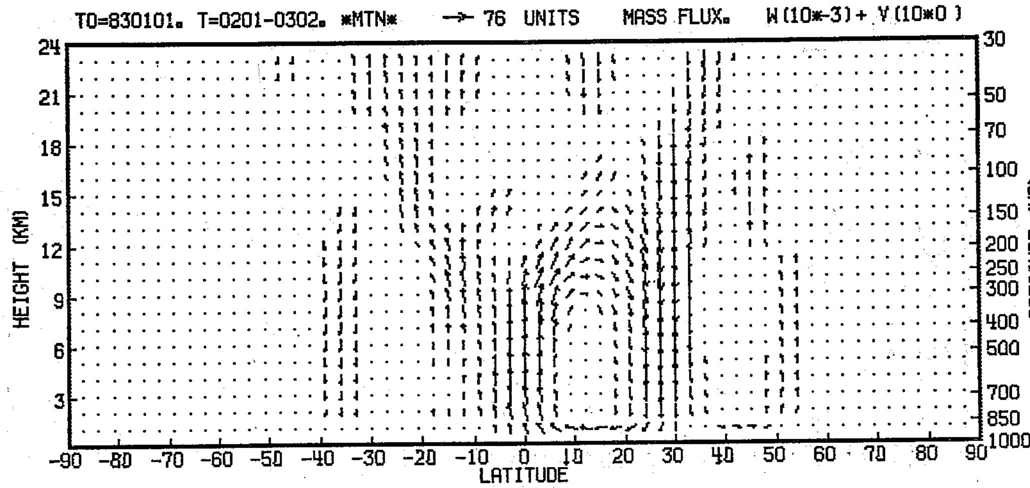

Fig. B.1 ($\overline{v}$,$\overline{w}$) [B1]

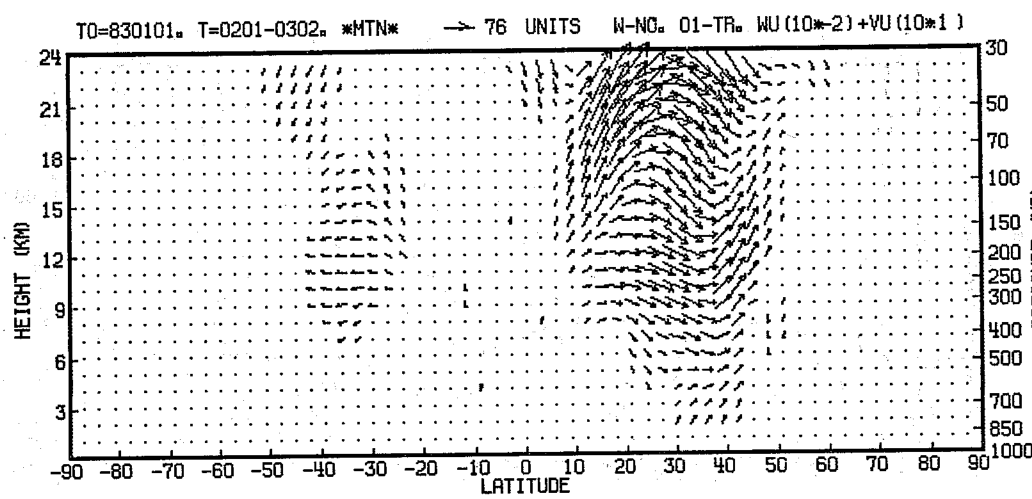

Fig. B.2 ($\overline{vu}$,$\overline{wu}$) by all eddies [B4]

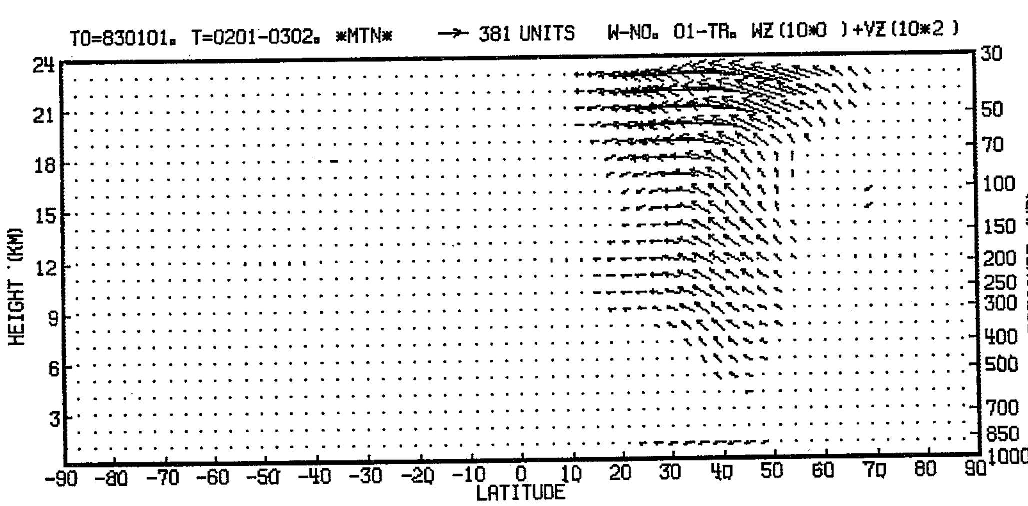

Fig. B.3 ($\overline{vz}$,$\overline{wz}$) by all eddies [B9]

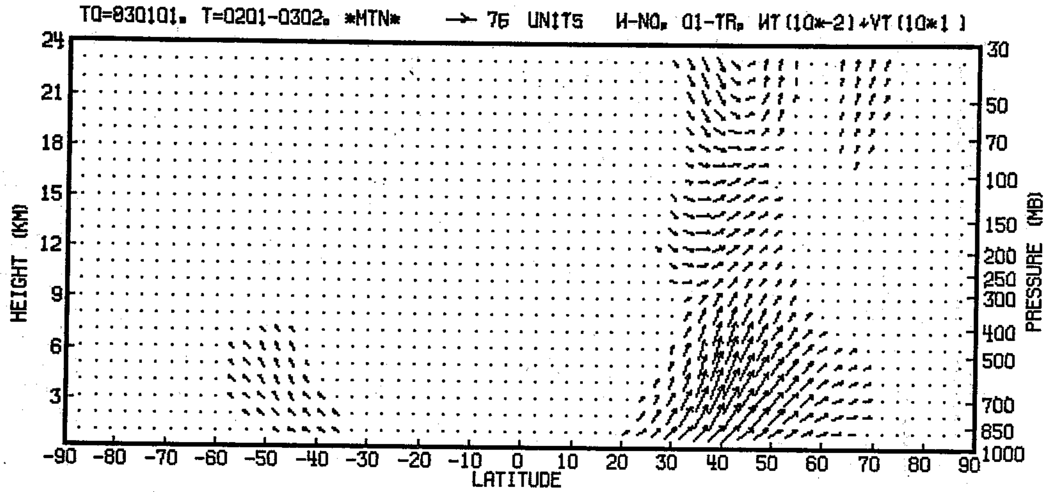

Fig. B.4 ($\overline{vT}$,$\overline{wT}$) by all eddies [B12]

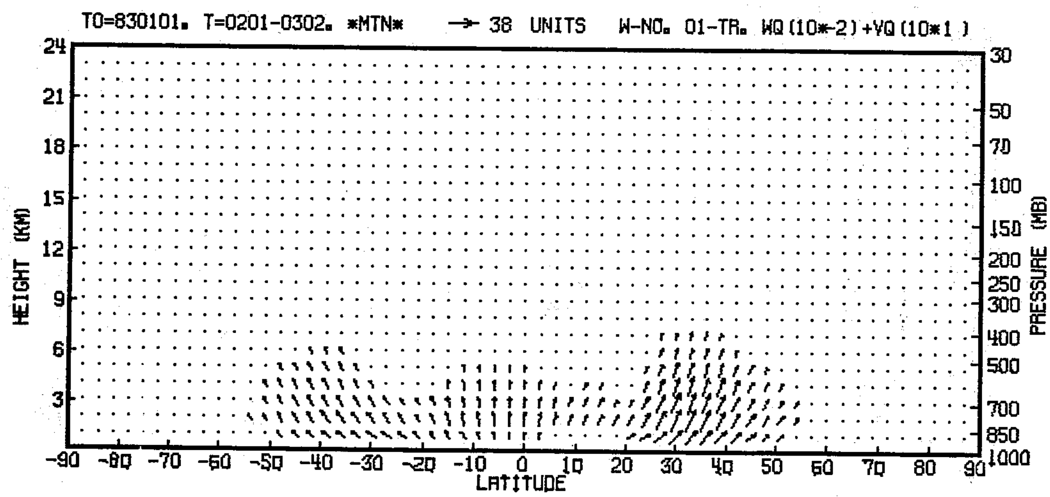

Fig. B.5 ($\overline{vq}$,$\overline{wq}$) by all eddies [B17]

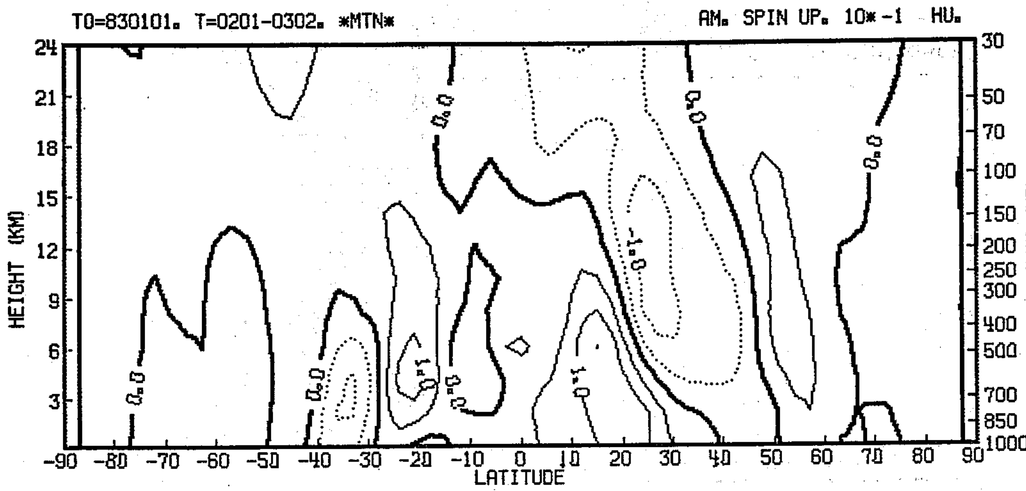

Fig. C.1 Spin-up of the zonal flow [C1]

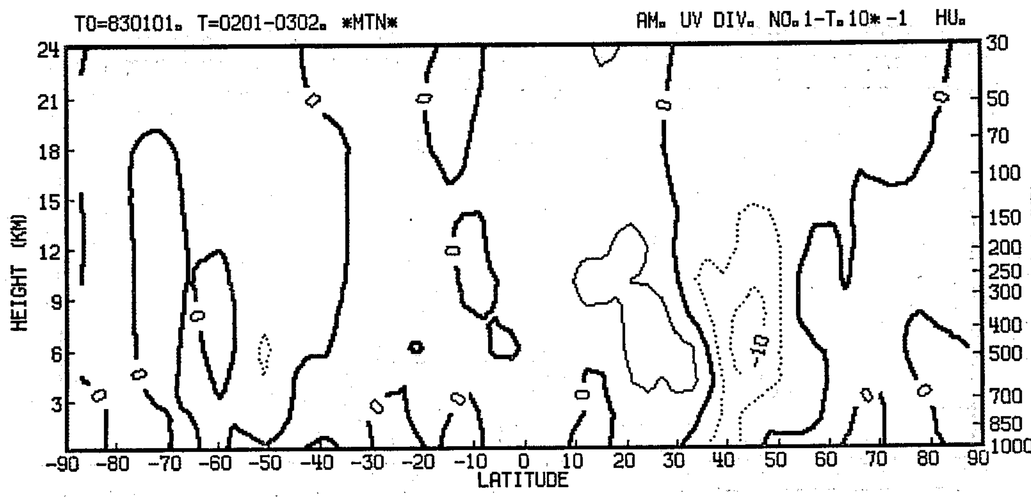

Fig. C.2 Horizontal divergence of the horizontal angular momentum flux due to all eddies [C4]

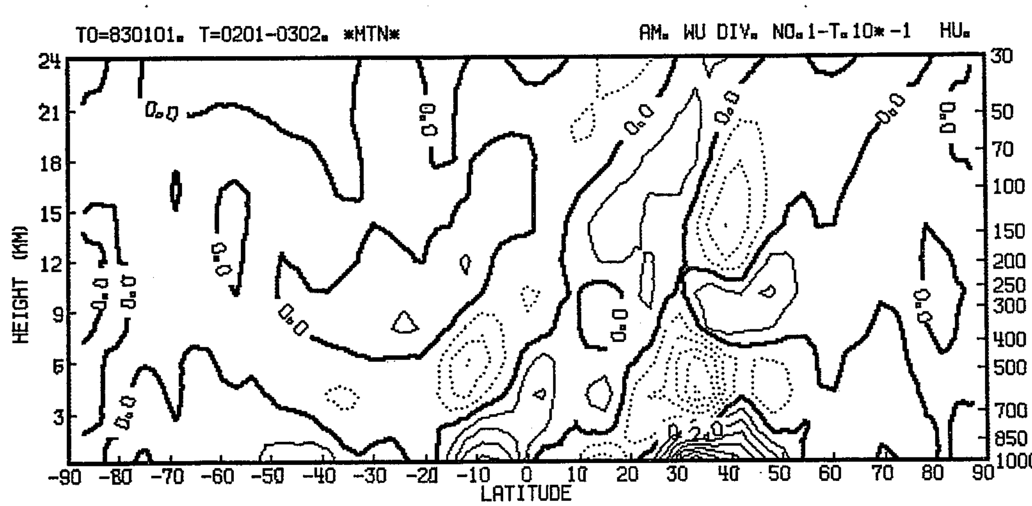

Fig. C.3 Vertical divergence of the vertical angular momentum flux due to all eddies [C8]

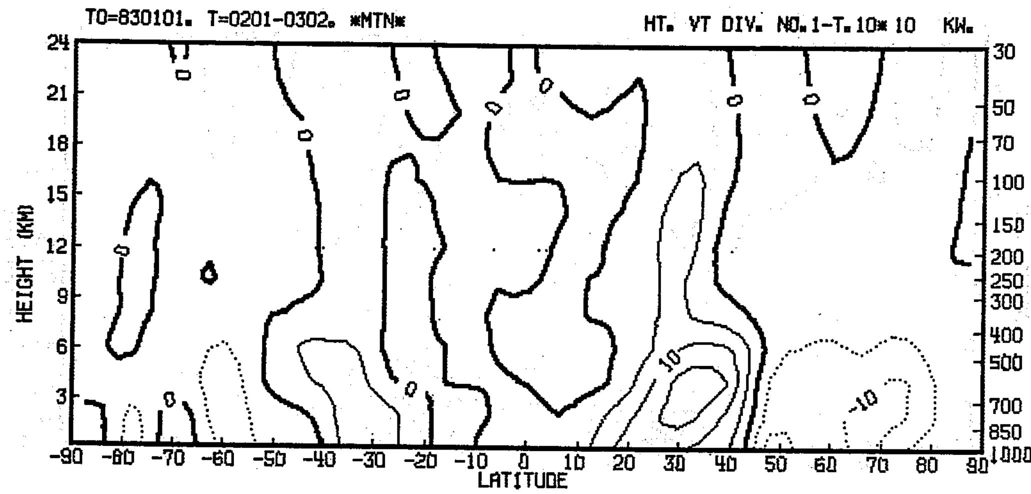

Fig. C.4 Horizontal divergence of the horizontal heat flux due to all eddies [C15]

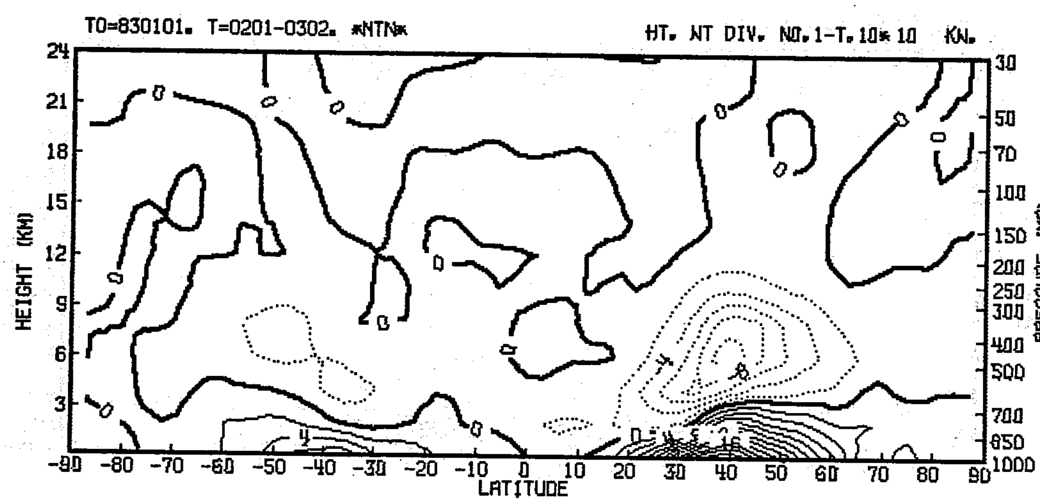

Fig. C.5 Vertical divergence of the vertical heat flux due to all eddies [C19]

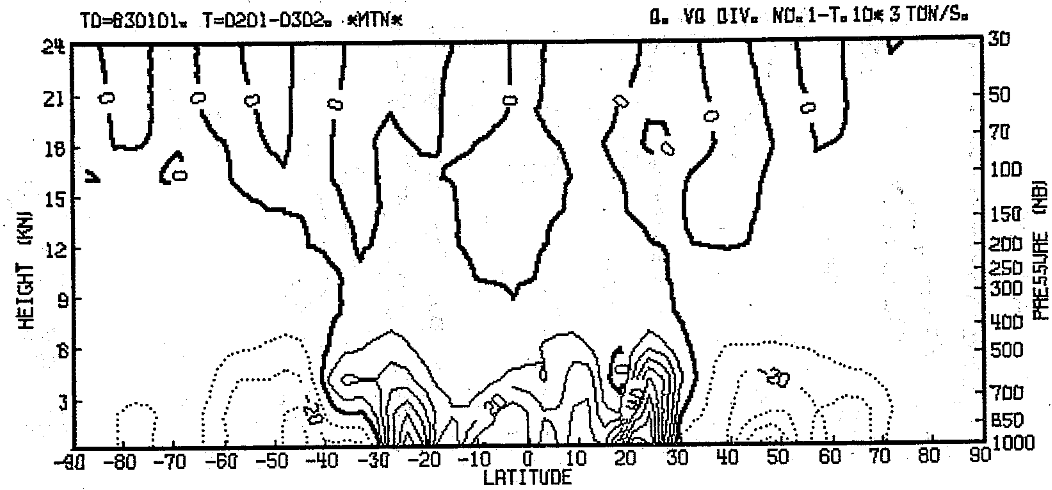

Fig. C.6 Horizontal divergence of the horizontal water flux due to all eddies [C26]

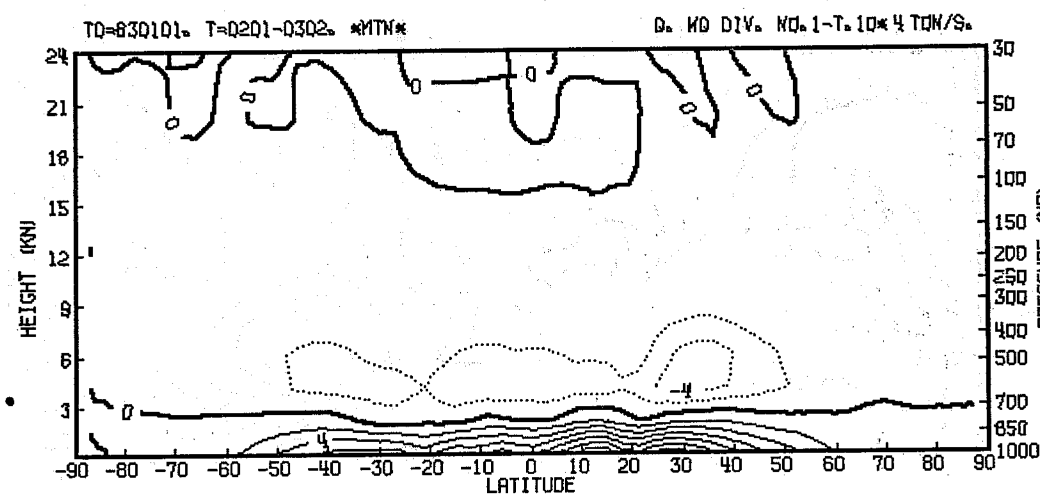

Fig. C.7 Vertical divergence of the vertical water flux due to all eddies [C30]

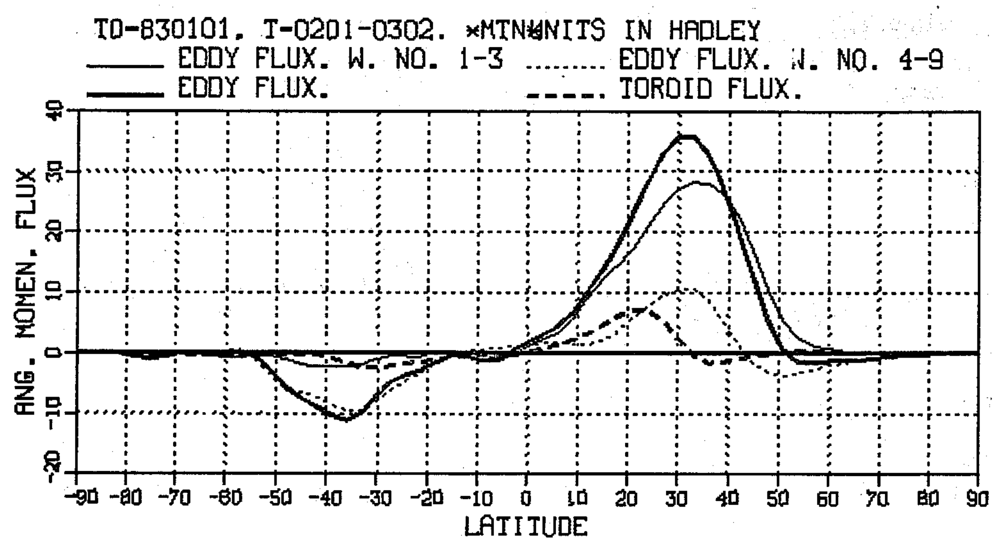

Fig. D.1 Vertically integrated horizontal angular momentum fluxes [D1]

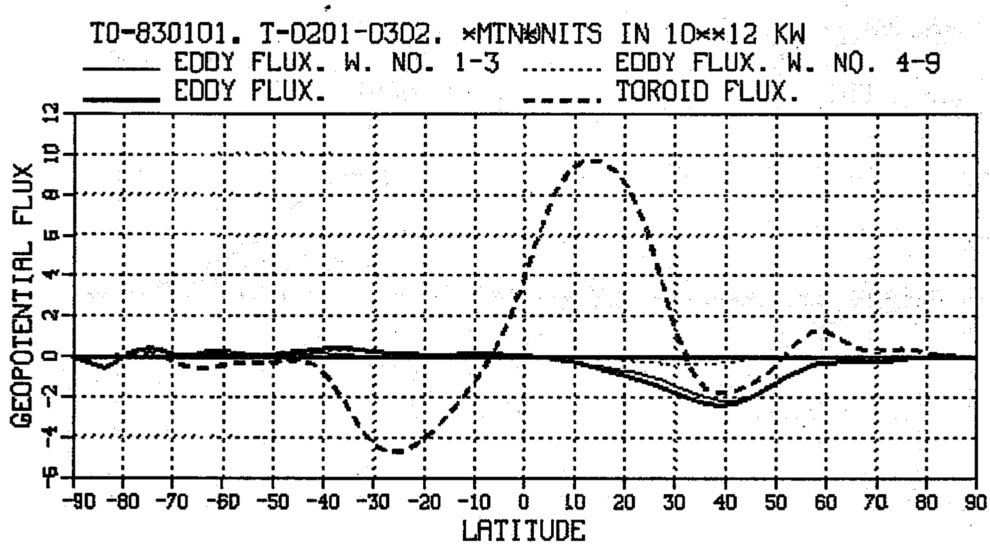

Fig. D.2 Vertically integrated horizontal geopotential fluxes [D2]

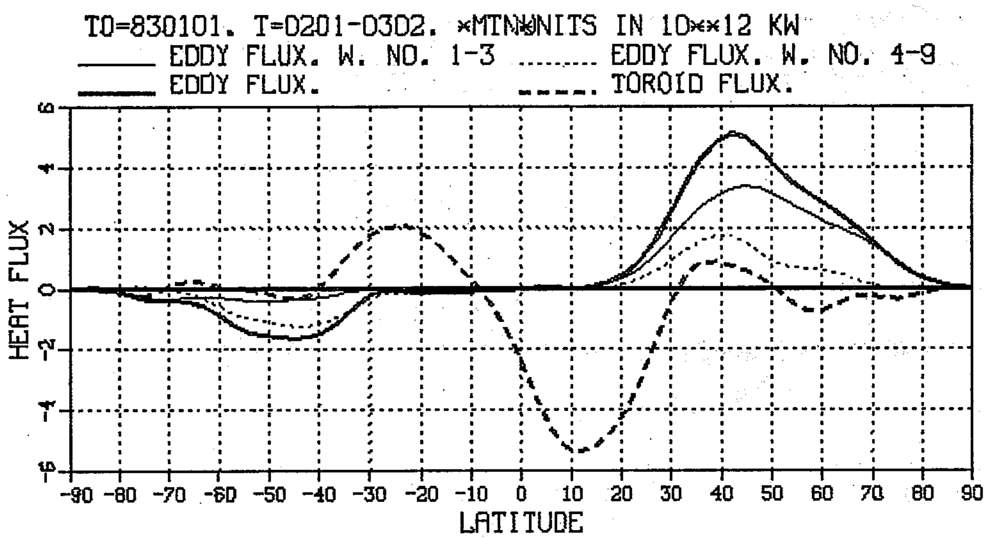

Fig. D.3 Vertically integrated horizontal heat fluxes [D3]

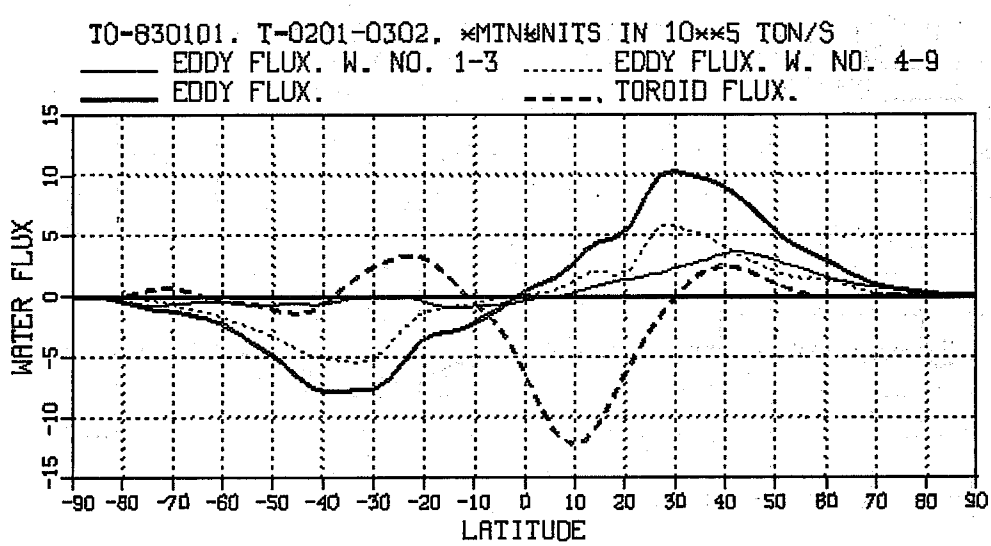

Fig. D.4 Vertically integrated horizontal water fluxes [D4]

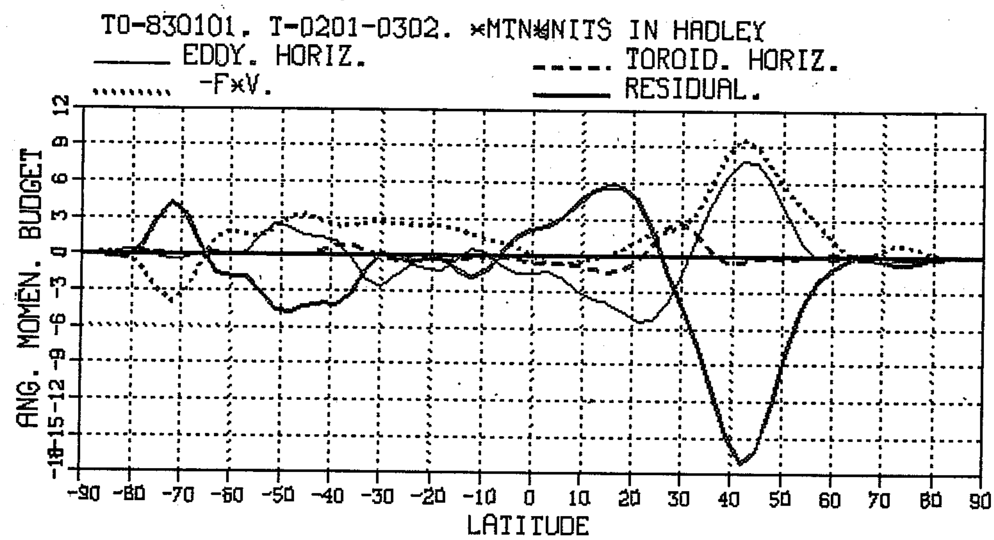

Fig. D.5 Vertically integrated angular momentum budget [D5]

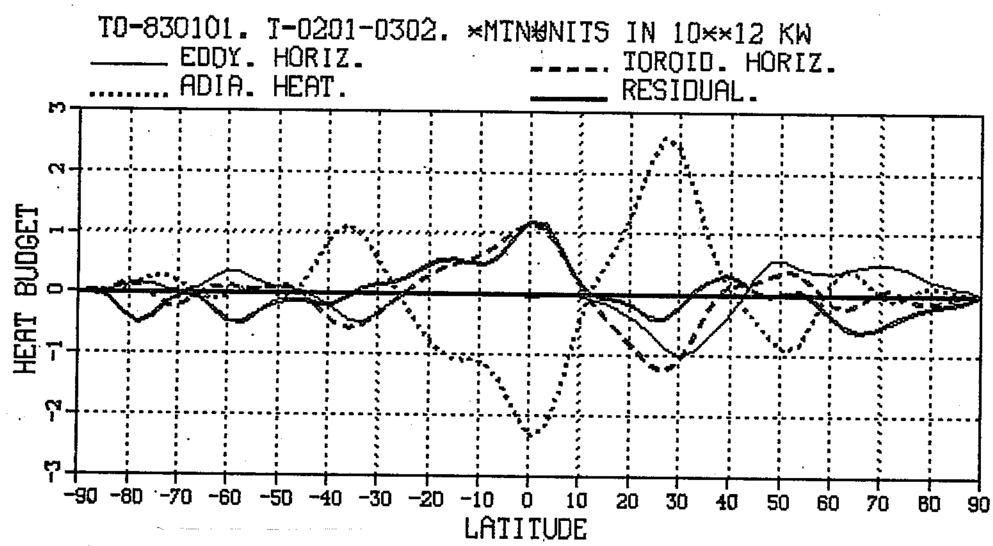

Fig. D.6 Vertically integrated heat budget [D6]

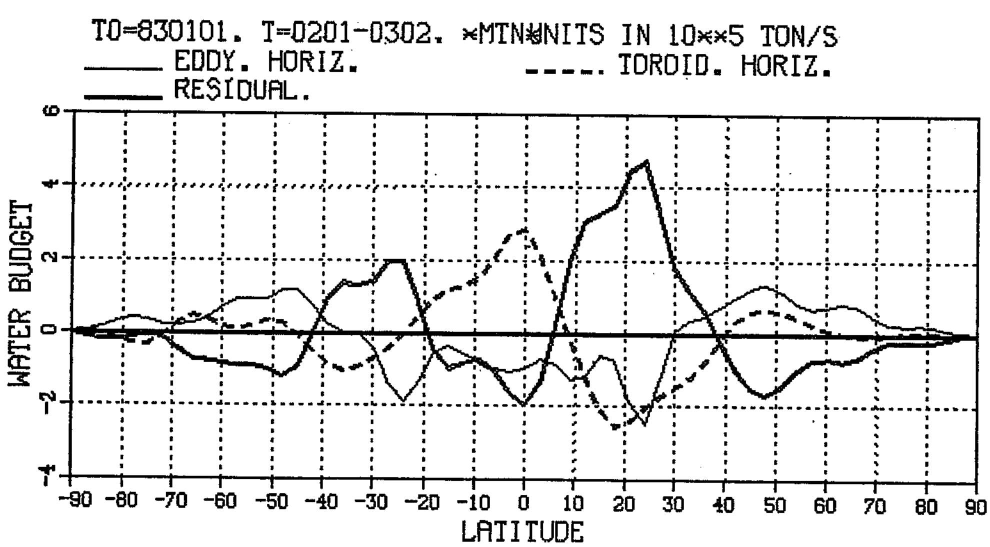

Fig. D.7 Vertically integrated water budget [D7]